FBG-based ultrasonic wave detection and acoustic emission linear location system*

JIANG Ming-shun(姜明顺)[1,2]**, **SUI Qing-mei**(隋青美)[1], **JIA Lei**(贾磊)[1], **PENG Peng**(彭蓬)[2], and **CAO Yu-qiang**(曹玉强)[1]

1. School of Control Science and Engineering, Shandong University, Jinan 250061, China

2. Yanzhou Coal Mining Group Co. Ltd., Postdoctoral Workstation, Zoucheng 273500, China

(Received 6 December 2011)

The ultrasonic (US) wave detection and an acoustic emission (AE) linear location system are proposed, which employ fiber Bragg gratings (FBGs) as US wave sensors. In the theoretical analysis, the FBG sensor response to longitudinal US wave is investigated. The result indicates that the FBG wavelength can be modulated as static case when the grating length is much shorter than US wavelength. The experimental results of standard sinusoidal and spindle wave test agree well with the generated signal. Further research using two FBGs for realizing linear location is also achieved. The maximum linear location error is obtained as less than 5 mm. FBG-based US wave sensor and AE linear location provide useful tools for specific requirements.

Document code: A **Article ID:** 1673-1905(2012)03-0220-4

DOI 10.1007/s11801-012-1190-4

Fiber Bragg grating (FBG) sensors have been indicated as the ideal candidate for practical structural health monitoring[1]. Recently, high-frequency detection, including acoustic emission (AE) and ultrasonic (US) waves, is becoming an urgent problem in health monitoring sensing domain[2]. Perez et al[3] demonstrated the feasibility of AE detection using FBGs, and anomalous responses have been observed when the acoustic wavelength is obviously higher than the grating length. Then Fisher et al[4] found anomalous events by increasing the acoustic frequency while acoustic wavelength approached the grating length. The further research of Aldo Minardo et al[5] provided the detailed information for actual influence of US perturbation on the shape and central wavelength of the grating peak. Jung-Ryul Lee et al[6] designed an FBG AE sensor for mechanical tests.

In this paper, the response of FBGs to longitudinal US waves is theoretically analyzed first. FBG-based US sensors and interrogation system with tunable fiber laser are designed by using rational parameters configuration. The relevant standard sine wave and spindle wave tests are carried out, which use an aluminum panel as the transmission medium and a piezoelectric transmitter as the signal generator. And finally, an AE linear location system and experiments are achieved.

The FBG response of US wave model is illustrated in Fig.1. The FBG is fabricated by UV laser, and it is written into the SMF-28 fiber with grating length of L. The FBG wavelength under match condition is defined as

$$\lambda_{B0} = 2n_{eff\,0}\Lambda_0 \ . \tag{1}$$

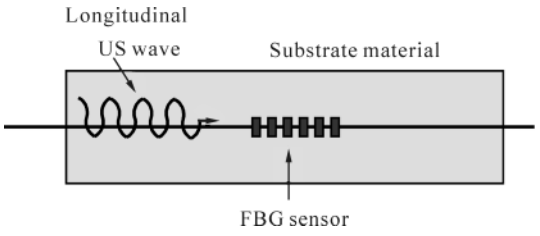

Fig.1 Schematic diagram of the FBG longitudinal response

Moreover, when the FBG receives the US wave, the grating can be described by a modulation of the effective refractive index of the fundamental guided mode along the fiber axis z:

$$n_{eff}(z) = n_{eff\,0} - \Delta n \sin^2(\frac{\pi}{\Lambda_0} z),\ z \in [0, L] \ , \tag{2}$$

where n_{eff0} is the unperturbed effective refractive index, Δn is the maximum change of the refractive index, and Λ_0 is the

* This work has been supported by the National Natural Science Foundation of China (No. 61074163), the Natural Science Foundation of Shandong Province (No.ZR2011FQ025), and the Independent Innovation Fund of Shandong University (No.2010GN066).

** E-mail: sdujiangmingshun@163.com

grating period[7,8].

As shown in Fig.1, US wave travels along the fiber axis. The strain field is modeled by a longitudinal strain propagating along the fiber axis. The time dependence is assumed to be sinusoidal, and the US wave model can be expressed as

$$\varepsilon(t) = \varepsilon_{\mathrm{m}} \cos(\frac{2\pi}{\lambda_{\mathrm{s}}} z - \omega_{\mathrm{s}} t) , \tag{3}$$

where for simplicity, ε_{m} denotes the US displacement amplitude normalized to the US wave number of $2\pi/\lambda_{\mathrm{s}}$, ω_{s} is its angular frequency, and λ_{s} is US wavelength.

The FBG, which is fixed on the substrate material, suffers the interaction of geometric effect and elasto-optic effect under US wave excitation. The FBG effective refractive index modulation under the US wave can be rewritten as

$$n'_{\mathrm{eff}}(z',t) = n_{\mathrm{eff}\,0} - \Delta n \sin^2\left\{\frac{\pi}{\Lambda_0} f^{-1}(z',t)\right\} - (\frac{n^3_{\mathrm{eff}\,0}}{2})\times$$
$$[P_{12} - \nu(P_{11}+P_{12})]\cdot\varepsilon_{\mathrm{m}} \cos(\frac{2\pi}{\lambda_{\mathrm{s}}} z' - \omega_{\mathrm{s}} t) , \tag{4}$$

where P_{ij} are the stress-optic coefficients, and ν is the Poisson's ratio[9,10].

As can be see in Eq.(4), the effective refractive index n'_{eff} has a complex form due to nonuniform distribution of strain along the grating length. However, when the US wavelength λ_{s} is much greater than grating length L, Eq.(4) can be simplified. Hence, for $\lambda_{\mathrm{s}}/L >> 1$, a new Bragg grating description can be expressed as

$$n'_{\mathrm{eff}\,0}(t) = n_{\mathrm{eff}\,0} - \frac{n^3_{\mathrm{eff}\,0}}{2}\cdot[P_{12} - \nu(P_{11}+P_{12})]\cdot\varepsilon_{\mathrm{m}}\cos(\omega_{\mathrm{s}} t) , \tag{5}$$

$$\Lambda'_0(t) = \Lambda_0 \cdot [1 + \varepsilon_{\mathrm{m}} \cos(\omega_{\mathrm{s}} t)] . \tag{6}$$

Combining FBG wavelength decision condition:

$$\lambda_{\mathrm{B}}(t) = \lambda_{\mathrm{B}0} + \Delta\lambda_0 \cos(\omega_{\mathrm{s}} t) , \tag{7}$$

where $\Delta\lambda_0$ is the amplitude of the FBG wavelength modulation induced by the US wave, it can be expressed as

$$\Delta\lambda_0 = \lambda_{\mathrm{B}0}\varepsilon_{\mathrm{m}}\left(1 - (\frac{n^2_{\mathrm{eff}\,0}}{2})[P_{12} - \nu(P_{11}+P_{12})]\right) . \tag{8}$$

For $\lambda_{\mathrm{s}}/L >> 1$, the grating response in terms of a central wavelength shift is the same as that in the static case[11].

The designed FBG US sensing system is shown in Fig.2. A reliable and sensitive approach, based on tunable piezoelectric fiber laser interrogation and direct reflectometric demodulation, is adopted. The acoustic signals are actively generated by a PZT transducer, via an arbitrary waveform generator. The FBG sensor is glued to the aluminum panel (600 mm × 150 mm × 2 mm) surface with epoxy. In the attaching process, the FBG must be pre-strained to avoid dead-region of signal detection. The PZT is coupled to the surface of the panel in the FBG longitudinal direction. The tunable laser is connected to the FBG via a circulator, which directs the signal from the FBG to the photo-receivers. The isolator and the circulator can prevent the reflected light of FBG filter and FBG sensor from coming back to the light source. The output light power from the circulator is transformed by the photodiode into the electrical power which is processed by the computer. The laser wavelength is tuned to the left mid-reflection wavelength of the FBG to achieve ideal match demodulation[12]. Thus, the output power increases as the FBG sensor is elongated, while decreases as the FBG sensor is compressed.

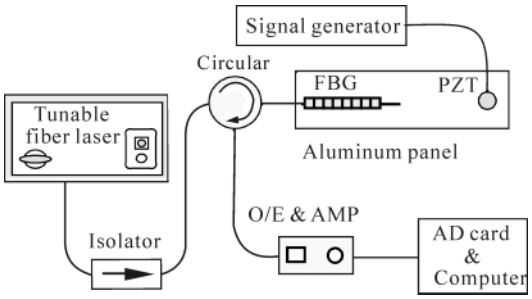

Fig.2 Experimental setup for the FBG-based US sensing system

The US propagation velocity in the aluminum plate is 5100 m/s. In experiments, the US frequency is set at 150 kHz. Thus we can induce that the US length is about 34 mm. According to the condition of $\lambda_{\mathrm{S}}/L >> 1$, the used FBG is fabricated by UV laser with the grating length of 5 mm (much shorter than the US wavelength) and the center wavelength of 1553.260 nm. And the reflection ratio is achieved to be 80%. In order to meet the requirement of interrogation system, the wavelength of tunable fiber laser is set at 1553.160 nm. And the output power is chosen as 10 mW. The standard technique for US wave excitation has been used, including a function generator, amplifier, and PZT actuator.

In this experiment, the waveform generator output is tuned at 150 kHz sinusoidal wave, with amplitude of 80 dB, burst of 10/ms, and rate of 100/pps. The PZT transducer is set at the FBG sensor longitudinal direction, and the distance between them is 200 mm. In addition, vaseline is used between the PZT transducer and the aluminum panel for increasing the excitation signal coupling degree.

Fig.3(a) shows the FBG time domain response. The time domain waveform agrees well with the set sinusoidal wave. Non-distortion detection is achieved. The frequency spectrum of the US wave detection can be constructed from taking the fast Fourier transform (FFT) from the time domain transient

response measured by the FBG US sensor, which is shown in Fig.3(b). The indicated peak of 150 kHz in the spectrum corresponds to the set frequency of the waveform generator. And the high signal-to-noise ratio (SNR) is obtained.

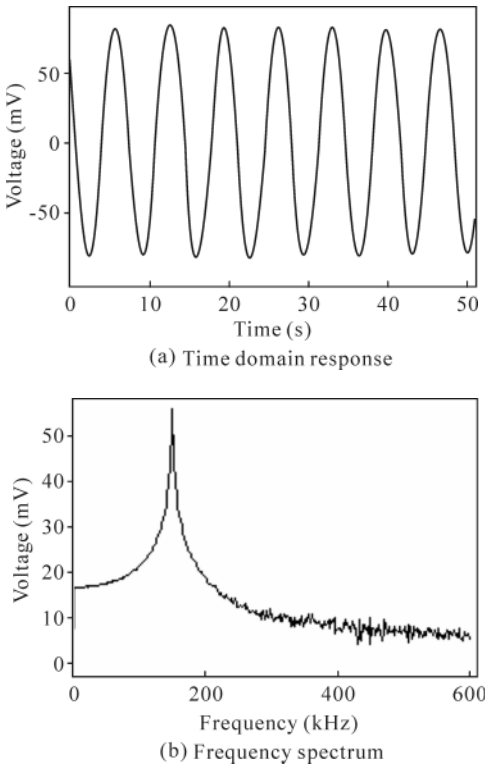

Fig.3 Longitudinal sinusoidal wave detection results using the FBG sensor

In order to test the spindle wave response of the FBG US sensor, the spindle pencil-lead breaking signal is simulated by the waveform generator. The main frequency is also set at 150 kHz. The detection system configuration is the same as that of the standard sinusoidal wave detection. Fig.4 shows the FBG sensor time domain response and frequency spectrum of the spindle wave, respectively. Whereas, as shown in Fig.4(b), concomitant noise is exhibited, which is due to the coupling degree between the PZT transducer and the aluminum panel, according to the analysis between experimental data.

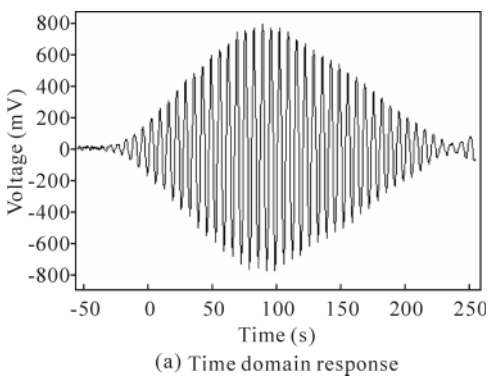

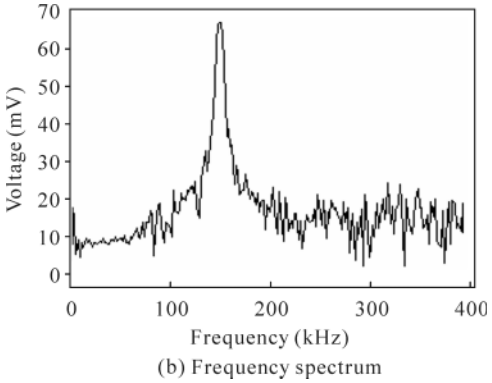

Fig.4 Longitudinal spindle wave detection results using the FBG sensor

In order to identify the AE location performance, the transient responses induced by the impact are measured by two FBGs simultaneously. The designed system is shown in Fig.5.

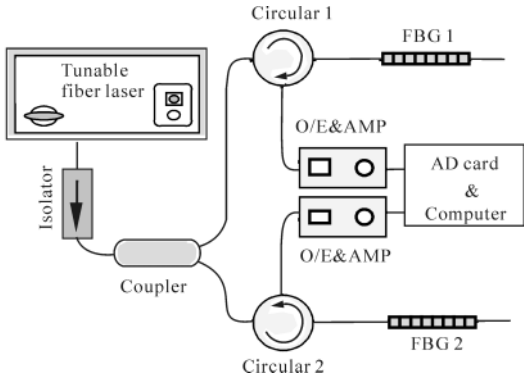

Fig.5 Experimental setup for the FBG-based AE location sensing system

FBG1 and FBG2 are fabricated under the same condition. The center wavelengths of them are 1553.260 nm and 1553.250 nm, separately. The tunable fiber laser is also set at 1553.160 nm to match the two FBG sensors. In order to perform the simultaneous measurement of the two FBG sensors, a 1 × 2 coupler is used to divide the light beam from broadband source into two paths. In Fig.6, the coordinate of AE location experimental aluminum panel is established. Suppose the left and under corner of the aluminum panel is the origin. This experimental region is chosen on the line where the width position is

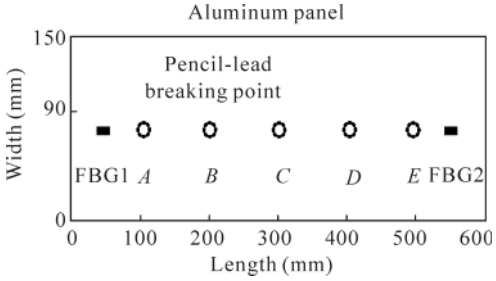

Fig.6 Experimental configuration for AE linear location

90 mm. The FBG1 and FBG2 are fixed at the points whose longitudinal coordinates are 50 mm and 550 mm, respectively.

Figs.7(a) and (b) are the time domain responses of FBG1 and FBG2, respectively under pencil-lead breaking at position *A*. As we can see, the response signal is received earlier in Fig.7(a) than Fig.7(b), because the pencil-lead breaking position *A* is closer to FBG1 than FBG2. Fig.7(c) shows the 3-D form of the FBG1 and FBG2 sensor detection. The difference between the two sensors can be distinguished directly. Then via data processing, the location point's longitudinal value of 96.4 mm is obtained.

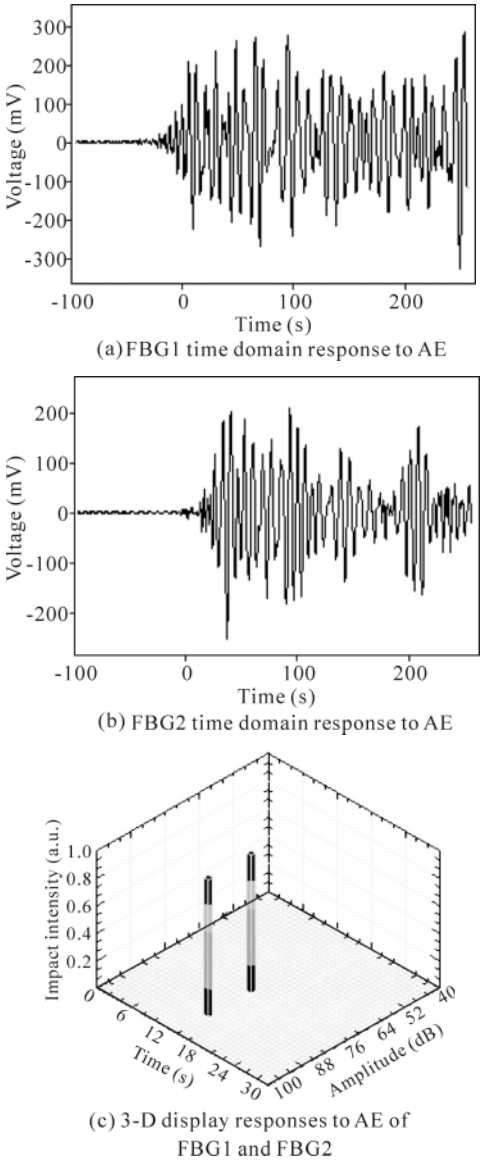

Fig.7 FBG1 and FBG2 detection results under pencil-lead breaking

In the following experiments, the pencil-lead breaking point is set at *B*, *C*, *D* and *E*, respectively. That is to say, its longitudinal coordinate value is 200 mm, 300 mm, 400 mm, and 500 mm, respectively. The experiment process is the same as that at the point *A*. The analysis results after date processing are shown in Tab.1. The maximum error is controlled in the range of ± 5 mm. The designed system provides a novel and high precision technique for AE location.

Tab.1 AE linear location results

	Pencil-lead breaking point	FBG US location system
A	100 mm	96.4 mm
B	200 mm	203.2 mm
C	300 mm	300.7 mm
D	400 mm	402.5 mm
E	500 mm	497.1 mm

In conclusion, the high-frequency dynamic responses of FBGs subjected to US wave and AE linear location are investigated. The interrogation scheme utilizing tunable narrow laser is verified. And location error less than 5 mm is obtained in the linear location tests. All the work is achieved based on the theoretical analysis of FBG sensor response to longitudinal US wave. In practice, AE surface and 3-D bulk location have extensive application foreground. Therefore, further research will regard the theoretical analysis of FBG to AE surface wave and cubic emission. And the diagnosis interrogation system is also prospected.

References

[1] JIANG Ming-shun, MENG Ling, SUI Qing-mei, PENG Peng and ZHAO Zeng-yu, Journal of Optoelectronics • Laser **22**, 1207 (2011). (in Chinese)

[2] GU Yi-ying, LI Shan-feng, LI Xin, LUO Xin, HAN Xiu-you and ZHAO Ming-shan, Journal of Optoelectronics • Laser **21**, 376 (2010). (in Chinese)

[3] I. Perez, H. L. Cui and E. Udd, Acoustic Emission Detection Using Fiber Bragg Gratings, SPIE **4328**, 209 (2001).

[4] N. E. Fisher, D. J. Webb, C. N. Pannell, D. A. Jackson, L. R. Gavrilov, J. W. Hang, L. Zhang and I. Bennion, Electron. Lett. **34**, 1139 (1998).

[5] A. Minardo, A. Cusano, R. Bernini, L. Zeni and M. Giordano, IEEE Transactions on Ultrasonics, Freeoelectrics, and Frequency Control **52**, 304 (2005).

[6] Jung-Ryul Lee and Hiroshi Tsuda, Scripta Materialia **53**, 1181 (2005).

[7] Graham Wild and Steven Hinckley, IEEE Sensors Journal **8**, 1184 (2008).

[8] Chien-Ching Ma and Cheng-Wei Wang, IEEE Sensors Journal **9**, 1998 (2009).

[9] C. Boulet, D. J. Webb, M. Douay and P. Niay, IEEE Photonics Technology Lett. **13**, 1215 (2001).

[10] Hiroshi Tsuda, Composites Science and Technology **66**, 676 (2006).

[11] B. Culshaw, G. Thursby, D. Betz and B. Sorazu, IEEE Sensors Journal **8**, 1360 (2008).

[12] H. Y. Ling, K. T. Lau, W. Jin and K. C. Chan, Opt. Commun. **270**, 25 (2007).